13th World Conference on Earthquake Engineering
Vancouver, B.C., Canada
August 1-6, 2004
Paper No. 920

NUMERICAL MODELING OF STRONG GROUND MOTION USING 3D GEO-MODELS

Peter KLINC[1], Enrico PRIOLO[1] and Alessandro VUAN[1]

SUMMARY

A procedure for an accurate computation of seismic waveforms in large-scale three-dimensional geomodels is presented. The procedure is based on the numerical modeling of the seismic waves propagation by means of a parallel implementation of the staggered grid Fourier pseudo-spectral method (FPSM). The adoption of FPSM is especially useful in addressing three-dimensional problems, because it requires a comparatively coarser sampling of the spatial domain. The considerable saving of the computer memory makes feasible an accurate description of the attenuation effects by means of the standard linear solid (SLS) model, which requires several variables defined over the computational domain. A further improvement of the computational efficiency is obtained by using Perfectly Matching Layer (PML) absorbing boundaries whereas accurate free surface condition are implemented at the top of the model. Thanks to the parallel implementation, we are able to model the seismic wave propagation in very large 3D geomodels, extending some hundreds of minimum wavelengths in each direction.
The finite seismic source effects are reproduced by a cinematic model of the rupture propagation along a fault plane. The planar source is simulated by summation of point sources distributed along a plane.
A validation with a reference method used for horizontally layered media has been carried out for a magnitude M=6 earthquake test case (the main shock of September 26, 1997, Umbria-Marche (Italy) event). An example is given, in which we improve the fit between the synthetic and the observed accelerogram by introducing a 3D heterogeneity in the structural model.

INTRODUCTION

Numerical simulations are helpful in seismic hazard analysis for two main reasons: 1) they allow to overcome the lack of empirical ground motion observations, 2) they are a tool for estimating the effects on the ground motion produced by particular features of the seismic source as well as of the geological structure. Recent studies suggest that long period ground motion estimation is significantly improved if 3-D structure is considered in the modeling (Olsen [1]; Kennett [2]).
However, the numerical simulation of seismic wave fields in three-dimensional large-scale complex models is computationally demanding and requires high performance parallel machines. The use of a

[1] OGS – Istituto Nazionale di Oceanografia e Geofisica Sperimentale, Trieste 34010, Italy. E-mail: pklinc@inogs.it

Fourier pseudo-spectral method (FPSM) for solving 3D problems (Reshef [3]) results in a coarser spatial sampling and improves the computational efficiency. The accuracy of the method is highly improved by evaluating the spatial derivatives on staggered grids, i.e. on separate grids which are shifted in space half a grid step along the direction of differentiation (Őzdenvar [4]).
Since the precise description of the macroscopic physical behavior of the earth medium does not allow independent consideration of the elastic response and of the attenuation properties (Minster [5]), the generalized standard linear model (Zener [6]) has been adopted for the description of the phenomenology of the earth medium and it has been embedded in the time domain computational scheme, by using memory variables (Carcione [7]). In order to minimize the wasted computational volume for the non-reflecting absorbing layers at the model boundaries, the Perfectly Matching Layers (PML) technique (Chew [8]) has been adopted. The free surface condition at the top boundary of the model has been introduced using an original approach designed for the FPSM.
The source finiteness effects may have a significant role in the strong ground motion distribution and it is compulsory to consider it in an earthquake scenario numerical simulation. The most direct approach to model it is to adopt a cinematic model of rupture propagation along a finite faulting surface and to reproduce it numerically with a weighted composition of point sources with delayed starting times.

METHOD

Modeling visco-elastic waves in 3D using a staggered grid parallel Fourier pseudo-spectral method

Equation of motion

The evolution of the seismic wavefield is computed in time domain and it is based on the equation of the momentum conservation, which is time stepped using the linearized form:

$$1)\ v_i(t+\Delta t) = v_i(t) + \frac{\Delta t}{\rho}\left(f_i^{ext.}(t+\frac{\Delta t}{2}) + \sum_{k=1,3} \sigma_{ik,k}(t+\frac{\Delta t}{2}) \right)$$

where $\boldsymbol{v}$ is particle velocity, ρ is density, $\boldsymbol{f}^{\,ext.}$ is the external force density, $\boldsymbol{\sigma}$ is the stress tensor and Δt is the time sampling interval.
The stress tensor evolution is time stepped using:

$$2)\ \sigma_{ij}(t+\frac{\Delta t}{2}) = \sigma_{ij}(t-\frac{\Delta t}{2}) + \dot{\sigma}_{ij}(t)$$

where the time derivative of the stress at time t has to be obtained from the spatial derivatives of the particle velocity field $\boldsymbol{v}(t)$ by applying a stress-strain relation.

Staggered grids scheme

The Fourier pseudo-spectral method requires a discretization of the spatial domain (a rectangular box) in a structured grid. The accuracy of the wave propagation modeling is highly improved by evaluating the spatial derivatives on separate grids of points which are shifted in space half a grid step along the direction of differentiation. Denoting the spatial Fourier transform along the p-th direction with F_p, the used differential operator can be expressed as:

$$3)\ D_p^{\pm} = F_p^{-1}\left[k_p \exp\left(\pm i k_p \frac{\Delta x_p}{2} \right) F_p \right]$$

The operators D_p^+ and D_p^- are applied alternately in order to produce the stagger instead of the drifting of the computational domain. Different components of the particle velocity field and of the stress field are therefore evaluated on different grids of points that are shifted in space half a grid step, as shown in Fig. 1. As a drawback of the adoption of the present scheme we find impossible the direct evaluation of the three components of the ground motion at the same point in space. In order to extract all the components of the ground motion at a receiver located in a reference grid node, we need to average the components evaluated in the nearest staggered grid points. Same applies for the perturbations of the stress field which are used to introduce the source.

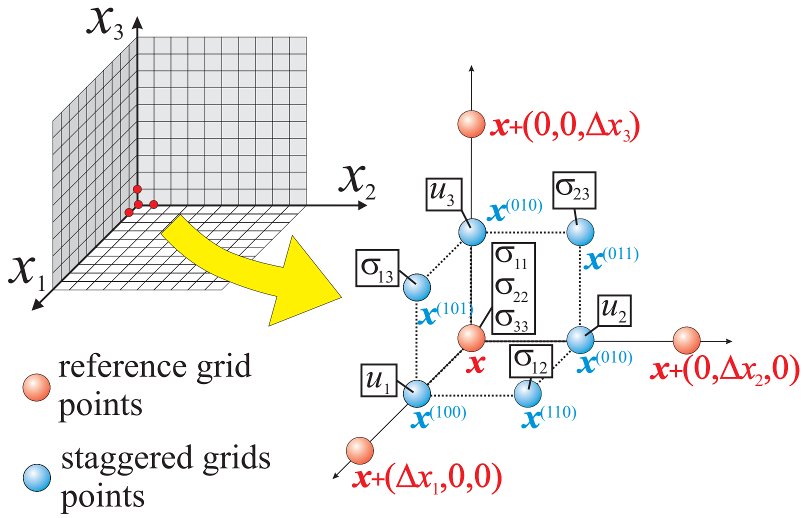

Figure 1: The staggered grids scheme

Modeling the attenuation

The stress response of a visco-elastic medium is characterized by the fading memory of the past strain states. With this concept in mind it is easy to overcome the awkwardness of the stress-strain relation for an isotropic visco-elastic solid which is usually written as:

3) $$\sigma_{ij} = \delta_{ij}\dot{\psi}_\lambda * \theta + 2\dot{\psi}_\mu * \varepsilon_{ij}$$

where δ_{ij} is the Kronecker's delta, ε_{ij} is the strain tensor, $\theta = \varepsilon_{11}+\varepsilon_{22}+\varepsilon_{33}$ is the dilatation and ψ_λ and ψ_μ are independent relaxation functions playing the role of the Lamé constants. Introducing $\psi_{\pi}= \psi_\lambda +2\ \psi_\mu$ as the P-wave relaxation function, we can rewrite eq. 3) as

4) $$\sigma_{ij} = \delta_{ij}\left(\dot{\psi}_\pi - 2\dot{\psi}_\mu\right) * \theta + 2\dot{\psi}_\mu * \varepsilon_{ij}$$

and we can describe the behavior of each of the P and S waves using the generalized standard linear (SLS) model:

5) $$\begin{cases} \psi_\pi(t) = (\lambda + 2\mu)\left(1 - \frac{1}{L}\sum_l a_l^P \exp\left(\frac{-t}{\tau_{\sigma l}^P}\right)\right)H(t) \\ \psi_\mu(t) = \mu\left(1 - \frac{1}{L}\sum_l a_l^S \exp\left(\frac{-t}{\tau_{\sigma l}^S}\right)\right)H(t) \end{cases}$$

where $H(t)$ is the Heavyside function, λ and μ are the "static" values of the Lamé constants, and a_l^S, $\tau^S_{\sigma l}$, a_l^S and $\tau^S_{\sigma l}$ are parameters to be evaluated separately from the desired frequency independent Q^P and Q^S using procedures which are not described here. The form of eq. (5) allows to rewrite eq. (4) as:

$$6)\ \sigma_{ij} = \delta_{ij}(\pi_0 - 2\mu_0)\theta + 2\mu_0\varepsilon_{ij} + \tfrac{1}{L}\sum_l R^{(l)}{}_{ij}$$

where $\pi_0 = \psi_\pi(0)$, $\mu_0 = \psi_\mu(0)$ and where $R^{(l)}{}_{ij}$ are the memory variables, which describes the stress contribution due to the past strain states. Thanks to the form of eq. (5) it is possible to implement a linearized time stepping scheme for the memory variables:

$$7)\ R^{(l)}_{ij}(t+\Delta t) = \left(1 - \frac{\Delta t}{\tau_{\sigma l}}\right) R^{(l)}_{ij}(t) + \Delta t\left(\delta_{ij}(\pi_l - 2\mu_l)\theta + 2\mu_0\varepsilon_{ij}\right)$$

with $\pi_l = (\lambda+2\mu)a_1^P/\tau_{\sigma l}$ and $\mu_l = \mu\, a_1^S/\tau_{\sigma l}$, having chosen $\tau_{\sigma l} = \tau_{\sigma l}^P = \tau_{\sigma l}^S$.
The described approach allows to model correctly the seismic waves propagation in media where the intrinsic attenuation of the compression waves is different from that of the shear waves, as demonstrated in Figure 2.

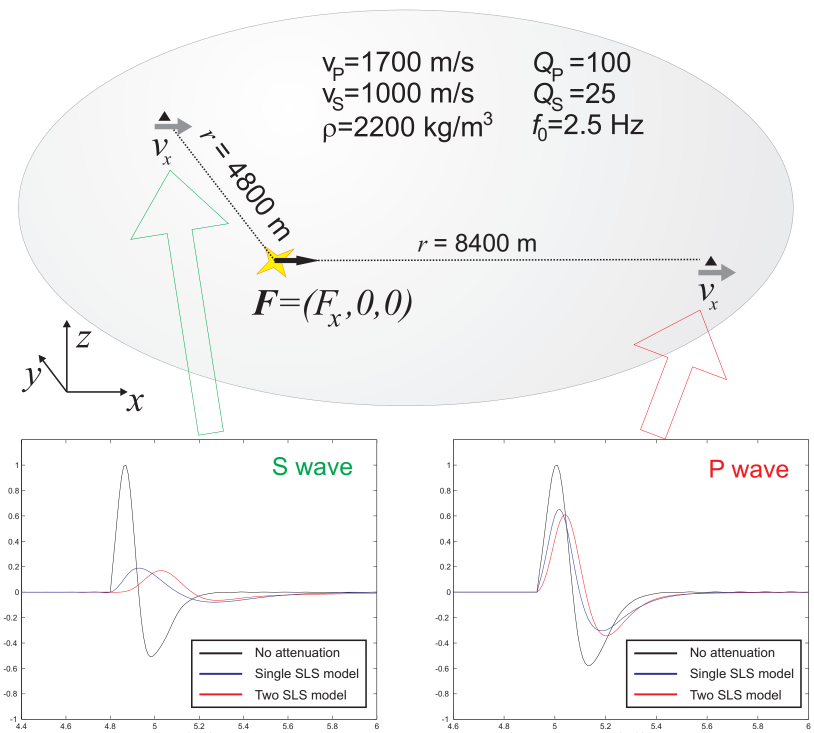

Figure 2: Effectiveness of the attenuation mechanism

Implementation of the parallel algorithm

The stress-velocity time advancing scheme is suitable for a parallel implementation. The massiveness of the data to be passed to the Fourier differential operators suggests a parallelization of the procedure following the data decomposition approach. The computational domain is evenly split into horizontal slices which are assigned to single processors. Each processor perform all the computations on the sub-domain that has been allocated to it except for the differentiation in the vertical direction. In order to compute the derivative in the vertical direction the computational domain is pro tempore re-organized in vertical slices (Figure 3). This step can be easily achieved in a Message Passing Interface (MPI) framework using the apposite MPI subroutine. Since the vertical derivatives has to be computed twice in a time step, a noticeable amount of communication between processors is required and the benefits from the parallelization can be lost if the computations are split in too many processors. Tuning tests are required to optimize the efficiency of the scheme and exploit at the best the computing power of the available multiprocessor device.

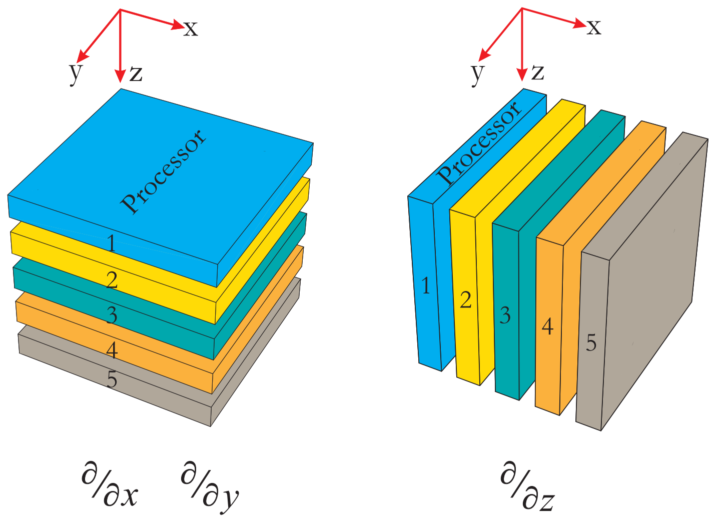

Figure 3: Domain decomposition approach

Model boundaries

Perfectly matching absorbing layers

In order to prevent the wrap-around effect (in the Fourier PSM the wavefield propagates through the model borders and comes back in the computational domain from the opposite side), the model must be surrounded by apposite absorbing layers. In 3D problems, the increase of the overall dimensions of the computational domain due to the application of classical sponge layers (Cerjan [9]) may be meaningful. On the other hand, the implementation of perfectly matched-layer – PML absorbing belts (Chew [8]; Collino [10]; Festa [11]), reduces the wasted computational domain to about 20% of that of the classical method.

The basic principle of the PML method is to surround the model with an unphysical damping medium which produces no reflections at the interface with the model. This can be achieved by forcing an anisotropic attenuation in the absorbing layer, setting it maximum for the waves entering perpendicularly the interface. See referenced works for theoretical details. In practice the wavefield in the absorbing layer is split in two parts: one propagating along the direction normal to the interface between the absorbing layer and the interior of the model, and the second one propagating in directions which are parallel to that interface. The PML method consists in an explicit damping of the normal part alone, whereas the other part evolves following the scheme adopted for the inside of the model.

Free surface

Usually the geo-models in which the wave propagation is simulated are bounded by a free surface on their top (x_3=0). The x_3-derivatives of the displacement and of the stress field at the free surface are to be evaluated as left derivatives (for x_3 increasing with depth). In order to simulate the value of the left x_3 derivative at x_3=0 using the Fourier global differential operator we need to define virtual particle velocity and stress fields above the free surface, i.e. in an additional layer below the bottom absorbing strip (consider the periodicity of the computational domain). The free surface condition:

8) $\begin{cases} \sigma_{q3} = 0 \\ R_{q3} = 0 \end{cases}$ for x_3=0

can be efficiently simulated with virtual σ_{q3} fields which are anti-symmetric around the free surface plane (image method, Levander [12]). On the other hand, the virtual particle velocity field in the region above the free surface must verify the condition:

9) $\begin{cases} v_{1,3} = -v_{3,1} \\ v_{2,3} = -v_{3,2} \\ v_{3,3} = -\frac{\pi_0 - 2\mu_0}{\pi_0}\left(v_{2,2} + v_{3,3}\right) \end{cases}$ for x_3=0

which is somewhat harder to impose. In the presented procedure the virtual particle velocity field above the free surface is described with a third degree polynomial with the four coefficients determined by imposing the continuity with the particle velocity field below the free surface and imposing the value of its derivative at x_3=0 using the equation (9).
The effectiveness of both the free surface and PML absorbing boundaries is illustrated in Figure 3. The formation of the Rayleigh wave and the vanishing of the wave-field exiting the computational domain as well as that of the wave-field wrapped around is clearly seen.

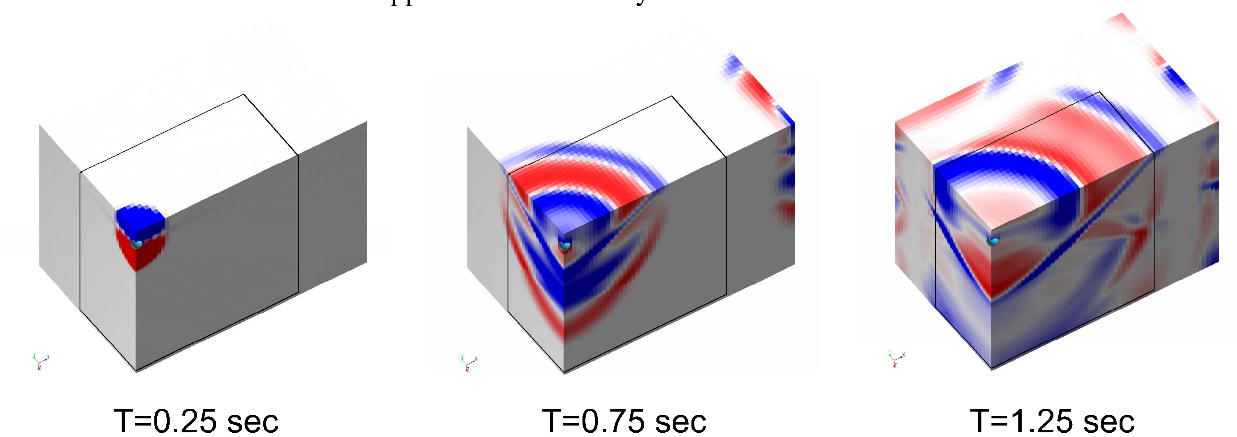

Figure 3: Effectiveness of the absorbing layers and free surface conditions

Modeling the fault surface
The earthquake source can be deterministically modeled to details corresponding to frequencies up to 1-2 Hz whereas higher frequencies require a stochastic approach, and are not considered here. Usually the deterministic forward modeling of earthquake ground motion at local distances is performed on the assumption that earthquake sources consist in a slip on a fault surface. This assumption allows to express the seismic representation theorem in terms of a surface integral. A popular approach in performing the surface integral is the point source summation (Hartzell [13]), in which the ground motion is evaluated as a sum of contributions from a set of point sources (hereafter source elements) which appropriately sample the fault surface:

11) $u_i(x_R, t) = \sum_n M_{jk}^{(n)}(t) * G_{ij,k}(x_R, t : x_S^{(n)}, 0)$

where $M_{jk}^{(n)}(t)$ is the seismic moment tensor time function of the n-th source element (which is a given parameter in the forward modeling) and $G_{ij,k}$ is the gradient of the Green's function (which has to be evaluated from the given geo-model).
In order to apply the point source summation technique in the framework of the presented FPSM, we select as elementary point sources locations a subset of reference grid nodes which are close to the defined fault surface. The fault surface is usually defined by its strike direction, dip angle, horizontal and down-dip extension and by the depth of its top margin.
Since the evolution of the slip along the fault surface typically follows a propagation of a rupture front from a postulated nucleation point (Heaton [14]), the elements are to be close enough each other in order to ensure the simulation of the continuity of the rupture process. Given the velocity of the seismic waves c, the velocity of the propagating rupture front v_R and the maximum considered frequency $f_{\max}$, the required spacing for the elements is (deduced from Hartzell et al. [13]):

$$12)\ \Delta r \leq \frac{c v_R}{2 f_{\max}\left(c + v_R\right)}$$

When the FPSM seismic wavefield simulation is performed using a single point source the spatial sampling of the computational domain is governed by the minimum wavelength. On the contrary, when simulating the wavefield due to a continuous rupture propagation on an extended source the more restrictive condition in equation (12) must be respected.
There are two approaches in which the presented staggered grid Fourier pseudo-spectral method for the seismic wave propagation modeling can be employed in the deterministic strong ground motion prediction. The direct approach consists in exciting the elements one after another, following a given rupture scenario and a given seismic moment distribution. This way it is possible to evaluate, with a single run, the evolution of the ground motion in the whole considered region, but only for the given scenario.
On the other hand there is the reciprocal approach, in which the FPSM is used to evaluate the gradient of the Green's function in the source elements locations by exploiting the reciprocity principle. This approach provides a database of Green's functions for the elementary sources locations and for a single observation point location. It can be used for an exhaustive study of different rupture scenarios effects but only at one observation point

TEST APPLICATION

Comparison with Wavenumber Integration Method

In the present work we test the deterministic modeling of the ground motion for a frequency up to 2Hz at local distances for a finite source by the described EXFPSM i.e. the direct modeling of the wavefield produced by a finite source using FPSM. The method is tested against a "classic" point source summation procedure we called EXWIM, (Priolo [15]) in which the elementary sources are located exactly on the fault surface and the Green's functions are computed by the Wavenumber Integration Method (WIM) using the software developed by Hermann [16]. The WIM solves the full-wave equation in anelastic media with a vertically heterogeneous (i.e. horizontally layered) structure.
The M_W=6.0 main shock of September 26, 1997, Umbria-Marche (Italy) earthquake is chosen as a reference for the test. The source model is defined following Capuano et al. [17], and consist in a plane fault surface 12 km long and 7.5 km wide, dipping with 38 degrees starting from a depth of 3.38 km. The slip distribution (with a total seismic moment release is $M_0=10^{18}$ Nm) is shown in Figure 4 and the rupture front is modelled considering the rupture propagation velocity v_R=2.6 km/s and a nucleation point near the lower right extremity of the fault surface. A constant value of -118 degrees has been assumed for the slip

direction (i.e. rake). Finite source synthetic seismograms were computed for the receiver locations corresponding to ENEA-ENEL accelerometric stations that recorded the event.

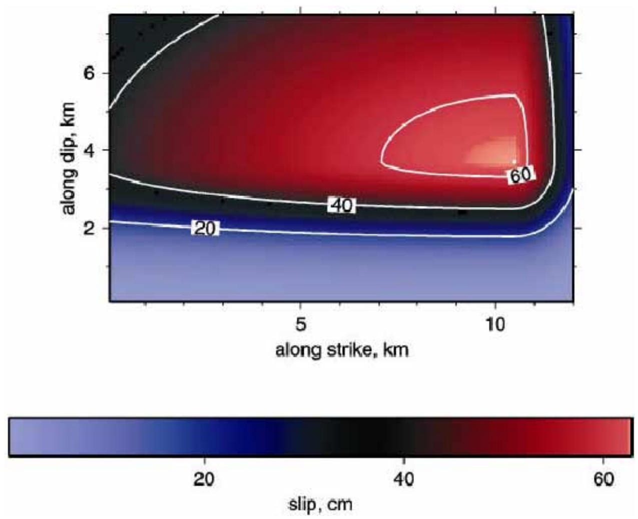

Figure 4: The modelled final slip distribution on the fault surface

The used structural model consists in the 5 horizontal layers defined in Table 1. Considering equation (12) we sampled the studied volume using a 200 m wide sampling step. The resulting structured grid contains 308 x 296 x 88 nodes not considering an 8 node wide PML boundary layer to be added at each side of the model except for the top.

Depth (km)	Vp (m/s)	Vs(m/s)	Density (kg/m3)	Qp	Qs
0-3	5080	2670	2560	290	100
3-5	5750	3030	2650	290	100
5-7	6000	3160	2800	290	100
7-15	6250	3300	2800	290	100
15+	6500	3420	2800	290	100

Table 1: The structural model used for the comparison between EXFPSM and EXWIM

A subset of 2299 nodes of the grid has been selected as elementary point sources on the basis of the geometrical description of the fault surface (Figure 5). To each of the nodes representing the elementary sources have been assigned a time delay corresponding to the arrival of the rupture front to the projection of the grid node on the fault surface and a seismic moment corresponding to the slip distribution in Figure 4. The field has been excited using delayed stress perturbations in the elementary point sources corresponding to the considered fault mechanism and scaled to the assigned seismic moment values. The perturbation follows a time function having the form of a smooth impulse with f_{max}=2Hz.

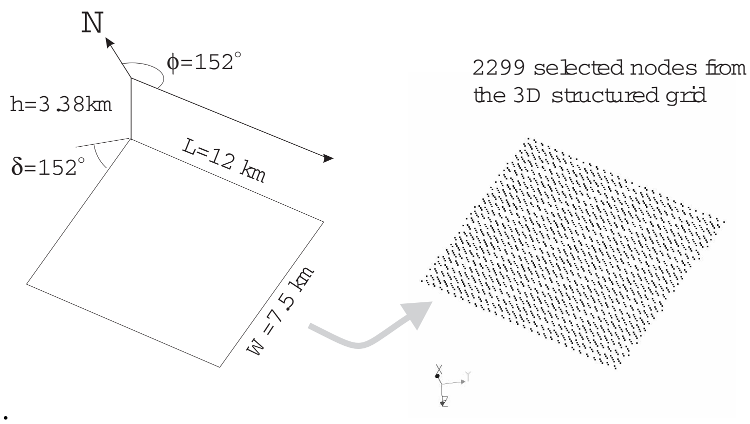

Figure 5: Representation of the fault surface with a selection of the 3D grid nodes

The run was performed using 22 processors of the IBM-SP4 supercomputer at CINECA, Bologna-Italy. The required 8000 time steps were computed in less than 6 hours. Some extracted snapshots (Figure 6) are very helpful for the understanding of the effects of the rupture propagation on the wavefield pattern.

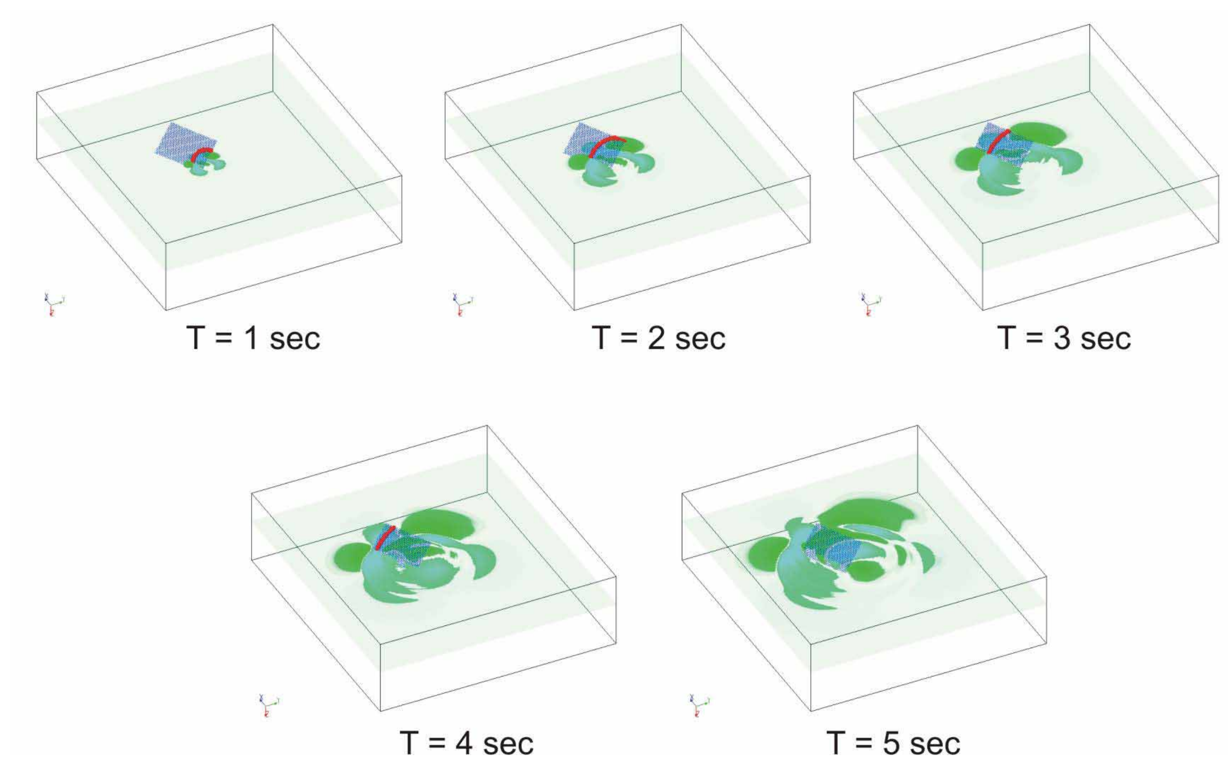

Figure 6: The seismic wavefield generated by the rupture propagation (red arc) along the fault.

The particle velocity waveforms extracted at the ENEA-ENEL accelerometric stations locations fits well both in amplitude and form with those obtained with the reference EXWIM method (Figure 7). The observed discrepancies are due to the fact, that the subset of grid nodes used in EXFPSM as elementary sources does not correspond to the elementary sources locations used by the EXWIM method. Anyway, the distances of the EXFPSM elementary sources from the reference fault plane are well inside the uncertainty level in the fault plane location for a forward modeling, thus we argue the strong ground motion prediction performed by EXFPSM is at least as much as accurate as EXWIM.

Figure 7: Comparison between waveforms computed using EXWIM (upper traces) and EXFPSM.

In order to illustrate the potentialities of the EXFPSM in predicting strong ground motion considering 3D heterogeneities we repeated the simulation using the structural model described in Table 1, but with a low velocity (v_P=2400 m/s, v_S=1250 m/s) lens extending 10 km across and 1 km in depth, just below the COLF station, aiming to reproduce the basin in which the station is located. The obtained acceleration waveform at COLF is far from fitting exactly the low pass (f_c=2Hz) filtered September 26, 1997 record, but it reaches the order of magnitude of the recorded amplitude values and returns a much more realistic complexity of the waveform than the simulation performed using the simple horizontally layered medium. With a more detailed definition of the structure beneath the considered station we would expect an even better fit.

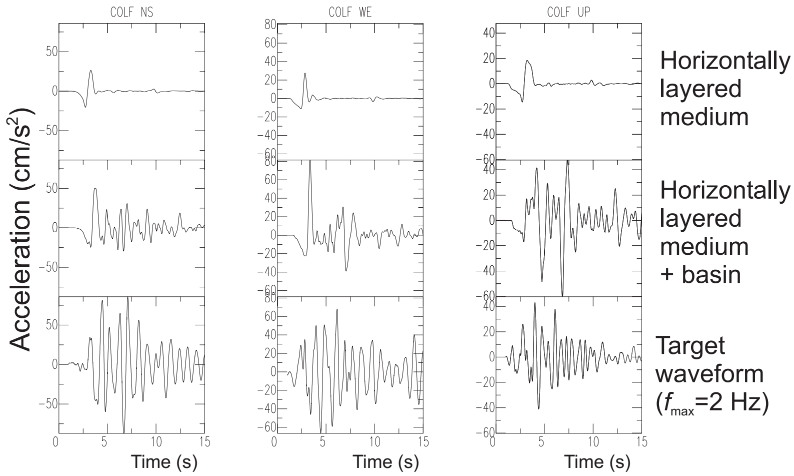

Figure 8: Comparison of the synthetics with the recorded accelerogram at station COLF

CONCLUSIONS

The described procedure allows the strong ground motion deterministic simulation (up to 1-2 Hz) on local distances considering at the same time a cinematic slip model for the finite source and a 3D complex viscoelastic structural model. A comparison with a reference method in a 1D model has been carried out for a realistic test case, providing a validation of the procedure. The simulations performed by including a three dimensional heterogeneity in the model (i.e. a sedimentary basin) gives more realistic waveforms compared to the results obtained using the horizontally layered structural model.

Further improvements of the method, such as the inclusion of topography effects, are planned.

REFERENCES

1. 1. Olsen KB and Archuleta RJ. "Three dimensional Simulation of Earthquake on the Los Angeles fault System." Bull. Seismol. Soc. Am. 1996; 86: 575-596.
2. Kennet BLN and Furumura T. "The influence of 3-D Structure on the Propagation of Seismic Waves Away from Earthquakes." Pure Appl. Geophys. 2002; 159: 2113-2131.
3. Reshef M, Kosloff D, Edwards M, Hsiung C. "Three-dimensional modeling by the Fourier method." Geophysics 1988; 53: 1184-1193.
4. Őzdenvar T and McMechan GA. "Causes and reduction of numerical artifacts in pseudo-spectral wavefield extrapolation." Geophys. J. Int. 1996; 126: 819-828.
5. Minster JB. "Wave propagation in viscoelastic media." Dziewonski AM, Boschi E, Editors. Physics of the Earth's Interior, Proceedings of the International School of Physics "Enrico Fermi", 1980; Course 78: 152-212.
6. Zener C. "Elasticity and Anelasticity of Metals". Univ. of Chicago Press, 1948.
7. Carcione JM, Kosloff D, Kosloff R. "Wave propagation in a linear viscoelastic medium." Geophys. J. Int. 1988; 95: 597-611.
8. Chew W, Liu QH. "Perfectly matched layer for the elastodynamics: a new absorbing boundary condition." J. Comp. Acoust. 1996; 4: 341-359.
9. Cerjan C, Kosloff D, Kosloff R, Reshef M. "A nonreflecting boundary condition for discrete acoustic and elastic wave equations." Geophysics 1985; 50: 705-708.
10. Collino F and Tsogka C. "Application of the perfectly matched absorbing layer model to the linear elastodynamic problem in anisotropic heterogeneous media." Geophysics 2001; 1: 294-307.
11. Festa G and Nielsen S. "PML Absorbing Boundaries." Bull. Seismol. Soc. Am. 2003; 93: 891-903.